Superconducting Current in Mesa Structures with Interlayer of Strontium Iridate, a Material Having Strong Spin-Orbit Interaction

A. M. Petrzhik[a, *], K. Y. Constantinian[a], G. A. Ovsyannikov[a], A. V. Shadrin[a, b],
Yu. V. Kislinskii[a], G. Cristiani[c], and G. Logvenov[c]

[a]*Kotel'nikov Institute of Radio Engineering and Electronics RAS, Moscow, 125009 Russia*
[b]*Moscow Institute of Physics and Technology, Dolgoprudny, Moscow oblast, 141700 Russia*
[c]*Max Planck Institute for Solid State Research, Stuttgart, 70569 Germany*
*e-mail: petrzhik@hitech.cplire.ru

Abstract—We report on observation of superconducting current and AC Josephson effect in mesa-hetero-structures with the interfaces comprised spin-singlet superconducting electrodes, coupled by a barrier made from strontium iridate, a material with the strong spin-orbit interaction. The superconducting critical current density was $j_C \approx 0.3$ A/cm^2 at $T = 4.2$ K for mesa-heterostructures with $d = 7$ nm and $j_C \approx 4$ A/cm^2 for $d = 5$ nm. The zero-bias conductance peak has been observed due to low energy states originated at Sr$_2$IrO$_4$/YBa$_2$Cu$_3$O$_x$ interface. Under influence of weak magnetic field the critical current $I_C(H)$ dependences showed Fraunhofer-like pattern indicating absence of pinholes, supported also by oscillating with microwave power Shapiro steps. Fiske resonance steps with voltage positions deviated from the ordinary ones were registered for mesas with $d = 5$ nm.

Keywords: interface, contact, iridate, heterostructure, superconductivity, Josephson effect, spin-orbit interaction, thin films

DOI: 10.1134/S1027451020030374

In recent years Josephson junctions featuring spin-dependent processes attract increasing interest. Particularly, spin-orbit interaction (SOI) in ferromagnetic (F) barrier material may lead to generation of spin-triplet superconducting current [1−5]. Theoretically magneto-electric effect and spin-triplet pairing were predicted for the case when ferromagnetic interlayer F was replaced by the normal-metal N with SOI [6, 7]. However, most of experimental investigations of impact of SOI on Josephson effect were performed in structures with superconductors linked by a topological insulator. A possibility to replace the topological insulator with a semiconductor film with SOI was suggested in [8] stimulating extensive theoretical and experimental studies [9, 10]. A promising choice of material with strong SOI for superconducting junction is the 5d transition-metal oxide Sr$_2$IrO$_4$ [11, 12]. This compound is known as a canted antiferromagnetic insulator with the band splitting, characterized by energy 0.4 eV [13]. Unconventional properties of Sr$_2$IrO$_4$ and the interfaces with other oxides, particularly with the superconducting cuprate, are discussed in refs. [14−16]. Moreover, Sr$_2$IrO$_4$ gives opportunities [17, 18] for spin manipulation in a junction with the

barrier material with weak magnetic moment. For experimental studies a sandwich-type structure seems promising due to the possibility to reduce the distance between superconductors down to a few nanometers that is necessary for the interference of superconducting wave functions in the junction. An inclusion of high-Z metallic Pt into the ferromagnetic interlayer for experimental study of impact of SOI on superconducting proximity effect was reported in [19].

In this report we present experimental results on observation of superconducting current and study of electron and microwave transport characteristics of hybrid superconducting Nb/Au/Sr$_2$IrO$_4$/YBa$_2$Cu$_3$O$_x$ sandwich-type mesa-structures with 5 and 7 nm thickness of the Sr$_2$IrO$_4$ interlayer.

For sample fabrication the bilayer of YBa$_2$Cu$_3$Ox (YBCO) and Sr$_2$IrO$_4$ (SIO) with thickness 60−70 nm and 5−7 nm, correspondingly, were grown epitaxially by pulsed-laser deposition (PLD) on (110) NdGaO$_3$ (NGO) single-crystalline substrates, as it was described in [16]. The superconducting Nb film with thickness about 200 nm was deposited ex situ by magnetron sputtering in an argon atmosphere at room temperature, followed after the sputtering of Au film
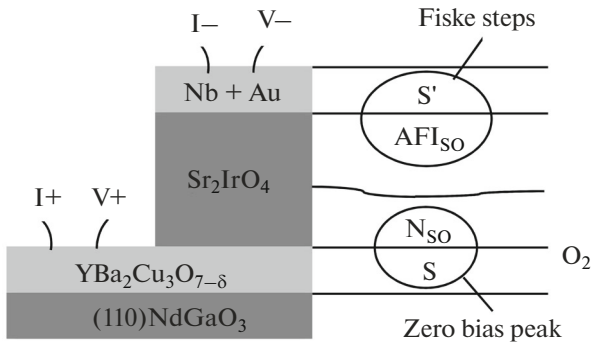
Fig. 1. A sketch of the mesa-heterostructure Nb/Au/SIO/YBCO on (110)NdGaO$_3$ substrate.

[20]. XRD data show that the lattice parameter $c = 1.283$ nm was obtained for SIO films and $c = 1.166$ nm for YBCO film. Nb/Au/SIO/YBCO mesa-structures (MS) with square shape and sizes $A = WL = 10 \times 10$ to 50×50 μm^2 (total 5 MS on a chip) were formed using optical lithography, reactive ion-plasma etching and ion-beam etching at low ion accelerating voltages (see Fig. 1).

After the structuring process the transition temperature of the YBCO electrode in the MS has reduced to $T_{C\_YBCO} \approx 61$ K, which could be explained by the influence of ion-beam etching and oxygen migration at SIO/YBCO interface. The normal state resistivity of Nb/Au interface, studied earlier [20], gave $R_N A = 10^{-6}$ μΩ cm^2, corresponding to a transparency $\Gamma \approx 1$. The averaged value of the normal resistivity for four MS on first chip with SIO thickness $d = 7$ nm was $R_N A \approx 10^{-4}$ Ω cm^2 and for second chip with $d = 5$ nm the averaged normal resistivity was $R_N A \approx 10^{-5}$ Ω cm^2. A model of tunnelling through a high resistive barrier is more applicable to the experimental data than a model of direct transport in the SIO interlayer. For the direct transport model an Ohmic dependency $R_N A(d) = \rho d$ where ρ is resistivity of SIO should take place. The SIO resistivity is higher than $\rho = 10^4$ Ω cm at 4.2 K that is clear from supplementary material to [21]. Taking $\rho = 10^4$ Ω cm the calculated value of resistivity by the Ohmic dependency one obtains of 7×10^{-3} Ω cm^2 for MS with $d = 7$ nm and of 5×10^{-3} Ω cm^2 for MS with $d = 5$ nm. It is much large than experimental values.

This allows to conclude that a tunnelling through high-resistive barrier takes place. This explains the measured value of $R_N A$ and allows to argue that the tunnelling is the main mechanism of electrical transport through the SIO/Au interfaces in the MS with a total transparency $\Gamma = 3 \times 10^{-5}$. Existence of zero-bias conductance peak (ZBCP), shown in Fig. 2, demonstrates that the SIO/YBCO interface also is transparent enough and low-energy states occurred. According to experimental data [22] even a minor change in the
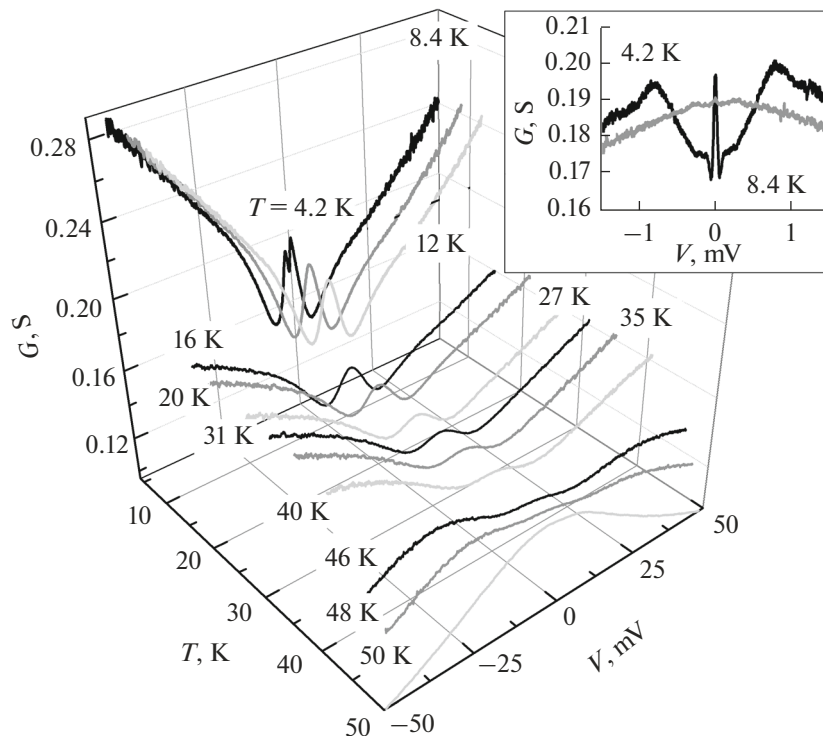
Fig. 2. Family of conductivity dependences $G(V)$ at temperatures $T = 4.2-50$ K.
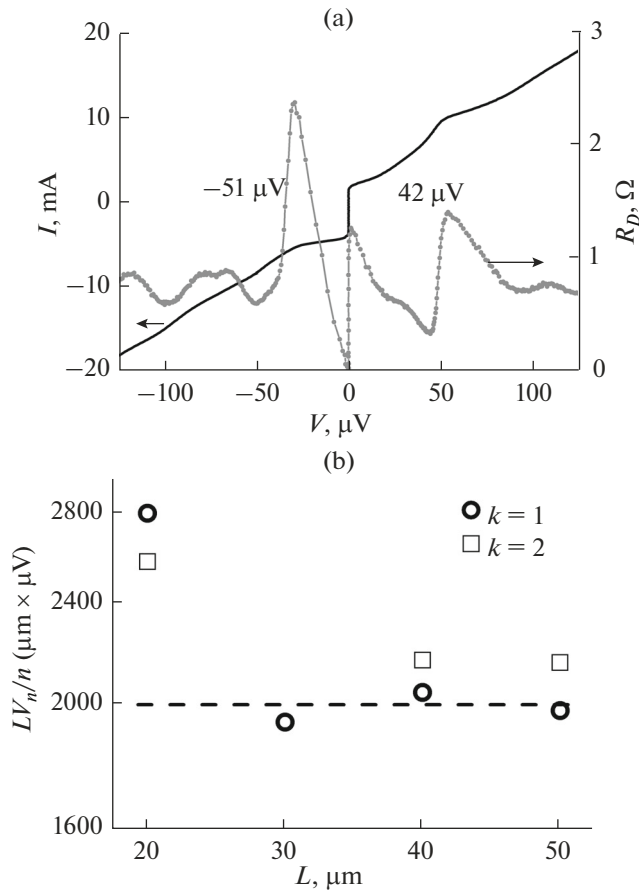
Fig. 3. I–V curve (solid black line), and $R_D(V)$ (grey line with dots) plotted at $H = -2.7$ Oe (a). Arrows point on Fiske resonance voltage positions for $k = 1$. The normalized by k the LV_k product vs. size L. Circles correspond to Fiske number $k = 1$, squares — to $k = 2$ (b).

oxygen content in SIO leads to a drastic change in the conductivity type at low temperature from activation to metallic. So, the interface SIO/YBCO could be considered as N_{SO}/S, where N_{SO} is a normal metal with SOI, and S is a singlet superconductor. Taking into account the rise of conductance $G(V)$ at $V > 10$ mV at low temperatures which is inherent to tunnelling and could be caused by an existence of insulating barrier I between SIO and Au/Nb superconducting S' bilayer, the whole MS could be modelled as $S'/I/N_{SO}/S$ (see Fig. 1).

In [21] it was shown, that the critical current of our mesa-structures increased with decreasing temperature similarly as the voltage of the energy gap singularity of Nb film. Under influence of magnetic field the critical current $I_C(H)$ dependences showed Fraunhofer-like pattern [21] indicating absence of pinholes, supported also by oscillating with microwave power Shapiro steps. Under electromagnetic radiation at millimetre wave frequency band, the Shapiro steps including the fractional ones were observed for mesas with $d = 7$ nm, indicating

the deviation of the current-phase relation from the sinusoidal and the presence of the second harmonic, which could not be explained solely by impact of d-wave symmetry of c-oriented YBCO electrode.

At voltages up to 200 μV (full range not shown in Fig. 3a) differential resistance $R_D(V)$ demonstrates oscillations which could be explain by Fiske resonances at $V_k = k(h/2e)c'/2L$, $c' = c(d/\varepsilon \, d_J)^{1/2}$ is Swihart velocity, $d_J = d + \lambda_{Nb}\text{ctanh}(d_{Nb}/2\lambda_{Nb}) + \lambda_{YBCO}\text{ctanh}(d_{YBCO}/2\lambda_{YBCO})\lambda_{YBCO} = 150$ nm and $\lambda_{Nb} = 90$ nm — London penetration depths for YBCO and Nb at 4.2 K. Changing the MS size the voltage positions of Fiske resonances changed as shown in Fig. 3b. Minor variation of expected V_kL products with changing L is seen, showed for the 1st and 2nd Fiske steps. At the same time the difference in V_{+1} and V_{-1} marked by arrows is seen well on $R_D(V)$ in Fig. 3a. An asymmetry has been observed also for higher k, as shown in Fig. 3b. Theoretical prediction of an asymmetry and deviation from ordinary Fiske resonance voltage positions were made in [22, 23] for the case of ferromagnetic insulator (IF, or IFI barriers) were mutual interaction of spin waves and plasma waves occurs. Spin waves in antiferromagnetic insulators are less studied, however their existence were examined in antiferromagnetic thin films [24], and antiferromagnetic spin dynamics in SIO was reported in ref. [25]. Fiske resonances were reported for Josephson junctions with metallic ferromagnets in IF barrier [26] without any deviation in V_k positions from ordinary theory [27]. A minor shift was noticed in ref. [28], which, however, could be explained by an influence of electromagnetic surrounding [29]. In our experimental case deviations are rather more pronounced. Furthermore, estimated from Fiske resonance position V_1 the plasma frequency $f_P \sim 25$ GHz gives high value of dielectric constant $\varepsilon \sim 40$–45, which does not contradict to values experimentally measured for SIO crystals [30] at somewhat higher temperatures than in our experiment and were explained by existence Mott band and strong SOI properties [31] in Sr_2IrO_4.

In conclusion, $Nb/Au/Sr_2IrO_4/YBa_2Cu_3O_x$ mesa-structures with epitaxial bilayer of Sr_2IrO_4 and $YBa_2Cu_3O_x$ films have been fabricated. The superconducting current for the thickness $d = 5$ and 7 nm of Sr_2IrO_4 interlayer has been registered. The zero-bias conductance peak has been observed and interpreted. Fiske resonances were registered for samples with $d = 5$ nm. From Fiske resonance positions dielectric constant $\varepsilon \sim 40$–45 was calculated.

FUNDING

REFERENCES

1. M. Eschrig, Rep. Prog. Phys. **78,** 104 501 (2015).

2. J. Linder and J. W. A. Robinson, Nat. Phys. **11,** 307 (2015).

3. F. S. Bergeret and I. V. Tokatly, Phys. Rev. B **89,** 134 517 (2014).

4. F. Konschelle, I. V. Tokatly, and F. S. Bergeret, Eur. Phys. J. **87,** 119 (2014).

5. F. S. Bergeret, A. F. Volkov, and K. B. Efetov, Rev. Mod. Phys. **77,** 1321 (2005).

6. I. V. Bobkova and A. M. Bobkov, Phys. Rev. B **95,** 84518 (2017).

7. C. R. Reeg and D. L. Maslov, Phys. Rev. B **92,** 134 512 (2015).

8. J. D. Sau, R. M. Lutchyn, S. Tewari, and S. Das Sarma, Phys. Rev. Lett. **104,** 040 502 (2010).

9. H. J. Suominen, J. Danon, M. Kjaergaard, et al., Phys. Rev. B **95,** 035 307 (2017).

10. D. Sun and J. Liu, Phys. Rev. B **97,** 035 311 (2018).

11. S. J. Moon et al., Phys. Rev. Lett. **101,** 226 402 (2008).

12. W. Witczak-Krempa, G. Chen, Y. B. Kim, and L. Balents, Annu. Rev. Condens. Matter Phys. **5,** 57 (2014).

13. Y. Gim, A. Sethi, Q. Zhao, et al., Phys. Rev. B **93,** 024 405 (2016).

14. S.-I. Hikino, J. Phys. Soc. Jpn. **87,** 074 707 (2018).

15. G. A. Ovsyannikov, A. S. Grishin, K. Y. Constantinian, et al., Phys. Solid State **60,** 2166 (2018).

16. A. M. Petrzhik, G. Christiani, G. Logvenov, et al., Tech. Phys. Lett **43,** 554 (2017).

17. H. Wang, S.-L. Yu, and J.-X. Li, Phys. Rev. B **91,** 165138 (2015).

18. Y. Chen and H.-Y. Kee, Phys. Rev. B **97,** 085155 (2018).

19. N. Satchell and N. O. Birge, Phys. Rev. B **97,** 214 509 (2018).

20. P. Komissinskiy, G. A. Ovsyannikov, K. Y. Constantinian, et al., Phys. Rev. B **78,** 024 501 (2008).

21. A. M. Petrzhik, K. Y. Constantinian, G. A. Ovsyannikov, et al., Phys. Rev. B **100,** 024 501 (2019).

22. O. B. Korneta, T. Qi, S. Chikara, et al., Phys. Rev. B **82,** 115117 (2010).

23. S. Mai, E. Kandelaki, A. F. Volkov, and K. B. Efetov, Phys. Rev. B **84,** 144 519 (2011).

24. M. Mori, S. Takahashi, and S. Maekawa, J. Phys. Soc. Jpn. **80,** 074707 (2011).

25. A. D. Boardman, S. A. Nikitov, and N. A. Waby, Phys. Rev. B **48,** 13 602 (1993).

26. S. Bahr, A. Alfonsov, G. Jackeli, et al., Phys. Rev. B **89,** 180 401 (2014).

27. A. Barone and G. Paterno, *Physics and Applications of the Josephson Effect* (Wiley, New York, 1982).

28. J. Pfeiffer, M. Kemmler, D. Koelle, et al., Phys. Rev. B **77,** 214 506 (2008).

29. R. Monaco, G. Costabile, and N. Martuccielle, J. Appl. Phys. **77,** 2073 (1995).

30. S. Chikara, O. Korneta, W. P. Crummett, et al., Phys. Rev. B **80,** 140 407 (2009).

31. J. Hu, Phys. Rev. Lett. **100,** 077 202 (2008).